Light Metals 2015
Edited by: Margaret Hyland
TMS (The Minerals, Metals & Materials Society), 2015

THE INFLUENCE OF CATHODE SHAPE ON CURRENT DENSITY AND METAL HEAVE IN 300 KA ALUMINUM REDUCTION CELL

Yang Song, Naixiang Feng, Jianping Peng, Baokuan Li, Qiang Wang
School of Materials and Metallurgy, Northeastern University, Shenyang, Liaoning 110819, China

Keywords: Inclined cathode, Cylindrical protrusions, Current density, Metal heave, Aluminum reduction

Abstract

A three-dimensional (3-D) model was developed to study the influence of cathode shape on current density, electromagnetic force and metal heave in 300 kA aluminum reduction cell. The new design is inclined cathode surface that makes horizontal current density in the metal pad as small as possible so as to simultaneously minimize power consumption. Results show that compared to plane cathode, cathode with 4.5° inclination can decrease 44.7 pct of horizontal current density. Cathode with 4.5° inclination and cylindrical protrusions can decrease 32.5 pct of horizontal electromagnetic force and 1.36 cm of metal heave in the metal pad.

Introduction

In a typical Hall-Héroult cell, current flows from anodes to metal through high-resistivity electrolyte in which alumina is dissolved [1]. Intense magnetic flux density (B) created due to high current in the busbars interacts with the current density vectors (J) flowing in the metal pad to generate magnetohydrodynamics (MHD) forces [2]. The MHD forces drive the metal flow and deform the metal pad so reduction of anode cathode distance (ACD) is constrained to avoid anodes immersed in the molten metal. The power is mostly consumed in electrolyte layer which has a relatively high resistivity. The aluminum industry is committed to increase MHD stability as greater stability of metal will aid in lowering ACD to save power consumption. At present one of the most urgent task is to achieve well-ordered electromagnetic force acting on melt flow in the cell.

Among much research on the topic, the most concern has been to improve busbar configuration and current distribution characteristics of components in aluminum reduction cell. Liang [3] reported comprehensive methods of busbar design from magnetic field compensation, busbar configuration, busbar section selection and short circuit in large aluminum reduction cells. Li [4] employed genetic algorithm for the numerical optimization of the busbar configuration based on MHD instability indicator. Gupta et al. [5] analyzed various busbar configurations and validated that new magnetic compensation effectively improves the magnetic field, metal flow profile and metal heave. Both W. Tao [6] and Y. Liu [7] simulated vertical collector bars in order to reduce the horizontal current and vertical magnetic field strength. Several designs have been adopted to compensate for external magnetic fields with side risers to reduce instability [8]. All these researches show satisfactory magnetic field improvement by optimizing busbar configuration. In other investigations, design modifications to cathode [9-15], collector bars [16], sidewall [8] were suggested in order to render the current density more uniform. Between improving busbar configuration and current distribution, the latter is more important. Even with a perfect busbar configuration, cell magnetic stability cannot be achieved without normal current distribution because uncontrolled change of current intensity in internal components can still affect electromagnetic forces and distort metal flow [17]. For existing cells, the busbar configuration can't easily be changed but current distribution improvement is possible by modifications of internal components during cell replacements.

The present paper investigates current density distribution and interface deformation from the point of cathode design. A 3-D model was established to investigate effect of various cathode inclinations on current density and inclined cathode with cylindrical protrusions on metal heave.

Mathematical model

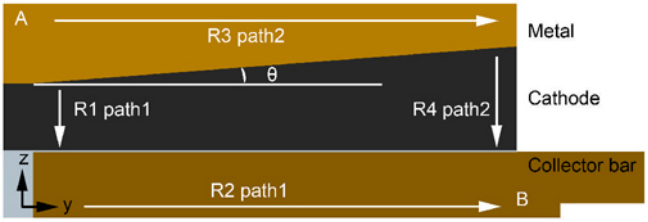

Figure 1. Sectional plane of inclined cathode assembly

Figure 1 represents the sectional plan of inclined cathode, proposed by Feng in 2011 [18]. Voltage drop between A and B is the same when current flows through path 1 or path 2.

$$I_1(R1+R2)=I_2(R3+R4) \tag{1}$$

$$\frac{I_2}{I_1}=\frac{R1+R2}{R3+R4} \tag{2}$$

$R1$, $R2$ resistance of cathode, collector bar in path 1.

I_1, I_2 current in path 1 and path 2.

$R3$, $R4$ resistance of aluminum, cathode in path 2.

θ cathode inclination

Resistance of aluminum is relatively small compared to cathode and collector bar, the equation is simplified to

$$\frac{I_2}{I_1}=\frac{R1+R2}{R4} \tag{3}$$

Increasing resistance of cathode in path 2 $R4$ will reduce horizontal current I_2 in aluminum if other parameters are constant. Using similar principle, Blais [15] changed bottom cathode design to reduce horizontal currents.

In this model, two stages for the current density and wave were adopted: First in ANSYS current density and Lorentz force are solved. Then in CFX velocity and interface deformation are solved using Lorentz forces found in first stage as source terms in the Navier-Stokes equations.

For electromagnetic analysis in ANSYS, electric potential V is solved from the Laplace equation.

$$\nabla \cdot (\sigma \nabla V) = 0 \tag{4}$$

where σ is electrical conductivity, V is electric potential.

The current density $\boldsymbol{J}$ is calculated from equation (5).

$$\boldsymbol{J} = -\sigma \nabla V \tag{5}$$

The magnetic field is calculated using Maxwell equations.

$$\nabla \times \boldsymbol{H} = \boldsymbol{J} \tag{6}$$

$$\boldsymbol{B} = \mu \boldsymbol{H} \tag{7}$$

where: $\boldsymbol{H}$ is magnetic field strength, $\boldsymbol{B}$ is the magnetic induction, $\boldsymbol{J}$ is current density, μ is permeability.

The Lorentz force resulting from interaction of the electromagnetic fields is given by the following:

$$\boldsymbol{F}_{EM} = \boldsymbol{J} \times \boldsymbol{B} \tag{8}$$

First the steady 3D electromagnetic field is solved and then we solve Navier-Stokes equation and k-ε turbulence equation to calculate flow field. The homogeneous VOF (Volume of Fluid) method was used for interface tracking [19].
Navier-Stokes equations:

$$\rho\left(\frac{\partial \boldsymbol{v}}{\partial t} + \boldsymbol{v} \cdot \nabla \boldsymbol{v}\right) = -\nabla p + \mu_{eff}\left(\nabla^2 \boldsymbol{v}\right) + \rho g + \boldsymbol{F}_{EM} \tag{9}$$

Where: $\boldsymbol{v}$ is velocity, p is pressure, μ_{eff} is effective dynamic viscosity, ρ is density; $\boldsymbol{F}_{EM}$ is electromagnetic force.

Continuity equation:

$$\nabla \cdot \boldsymbol{v} = 0 \tag{10}$$

k-ε turbulence models

$$\eta_t = c_\mu \frac{k^2}{\varepsilon} \tag{11}$$

k is turbulent kinetic energy, ε is turbulent kinetic energy dissipation rate.

$$\frac{\partial k}{\partial t} + (\boldsymbol{v} \cdot \nabla) k = \nabla \cdot \left[\left(\eta + \frac{\eta_t}{\sigma_k}\right)\nabla k\right] + \frac{G_k}{\rho} - \varepsilon \tag{12}$$

$$\frac{\partial \varepsilon}{\partial t} + (\boldsymbol{v} \cdot \nabla) \varepsilon = \nabla \cdot \left[\left(\eta + \frac{\eta_t}{\sigma_\varepsilon}\right)\nabla k\right] + \frac{C_{\varepsilon 1}\varepsilon}{\rho k} G_k - C_{\varepsilon 2}\frac{\varepsilon^2}{k} \tag{13}$$

Where η is kinematic viscosity, η_t is turbulent kinematic viscosity, σ_t, σ_ε, c_μ, $C_{\varepsilon 1}$, $C_{\varepsilon 2}$ are empirical constants, G_k is turbulent kinetic energy production item.

Four cathode inclination angles were compared to establish the extent of change to the current density: θ=0°, 3°, 4.5°, 6°.

The parameters in the calculations are in table I.

Table I. Calculation parameters

Parameters	Case 1	Case 2	Case 3
ACD (cm)	5		
Metal height (cm)	28		
Bath height (cm)	21.5		
Line current (kA)	300		
Cathode dimension (mm)	3420×525×490		

Results and discussion

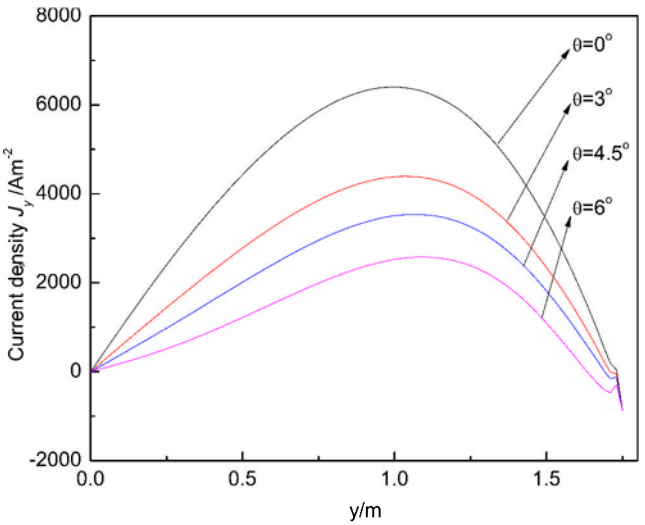

Figure 2. Y component of horizontal current density at 2/3 height of the metal pad

Figure 2 shows that y component of horizontal current density in the metal decreases with the increase of θ. The location of maximum wear and maximum current density at the surface of the block is matched [15]. Therefore, a decrease of current density will simultaneously reduce wear and prolong cathode life. This study found that cathode with 4.5° inclination decreased 44.7 pct of horizontal current density than plane cathode.

Horizontal current density in the metal was reduced with increased cathode inclination angle. Nevertheless, for the same metal level, metal volume is larger in the cell with 4.5° than with 6° cathode surface inclination. Since metal thermal stability would be better with more metal volume and having higher metal level above the protrusions would improve longevity, a 4.5° inclination was adopted to calculate flow field and wave. The following three cases were modeled:

Case 1: Traditional cell with plane cathode.

Case 2: Modified cathode with 4.5° inclination.

Case 3: Modified cathode with 4.5° inclination and cylindrical protrusions (Figure 3).

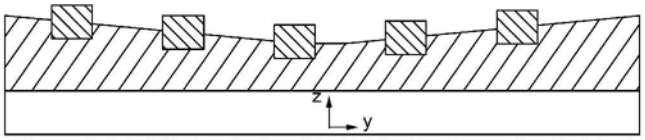

Figure 3. Modified cathode with 4.5° inclination and cylindrical protrusions

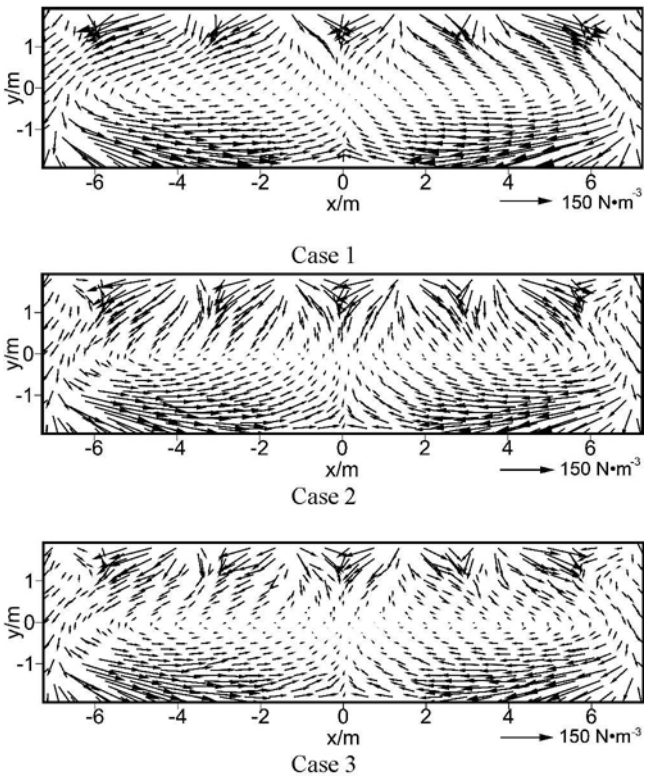

Figure 4. Horizontal electromagnetic force field at 2/3 height of the metal pad

Figure 4 shows horizontal electromagnetic force (HEMF) field at 2/3 height of the metal pad. The maximum HEMF was found to be 136 N/m3(case 1), 119 N/m3(case 2) and 92 N/m3(case 3) respectively. The HEMF is higher near the wall attributed to the presence of external vertical busbars. The decrease of HEMF can be explained by the corresponding lower current density attributed to cathode inclination and protrusions. The maximum horizontal electromagnetic force in case 3 was reduced by 32.5 pct compared to case 1.

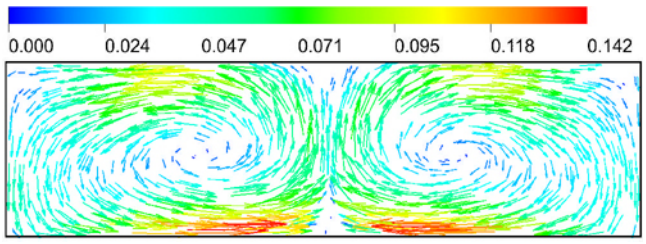

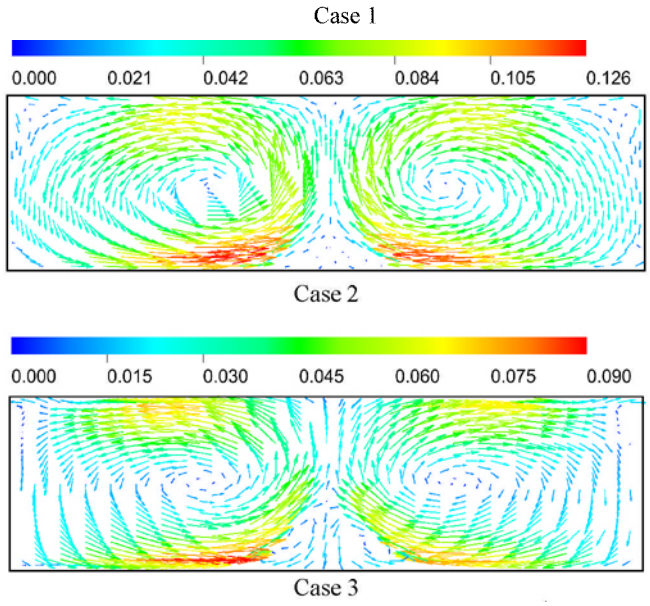

Figure 5. Flow field at 2/3 height of the metal pad (m•s^{-1}), t=100s

Figure 5 shows velocity at 2/3 height of the metal pad. There are two reverse vortices in the metal. Velocity decreases toward the center of the vortex. The match between the trend of HEMF and metal flow is noticeable. Cathode inclination and cylindrical protrusions reduced the metal flow, nevertheless, they didn't alter the flow pattern. The wave data is shown in table II.

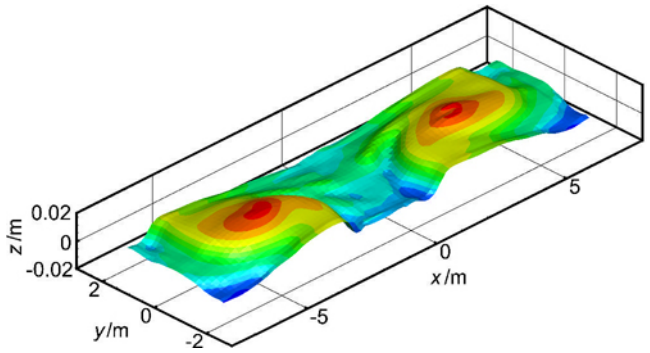

Figure 6. Bath-metal interface shape (m)

Figure 6 is bath-metal interface shape. The peaks of three cases are 1.89 cm, 0.68 cm, 0.56 cm. The electromagnetic force drives the metal flow and form two large heaves located near 1/4 and 3/4 length of the cell. The radial component of the electromagnetic force pushes the metal toward the center of the cell, which is the main cause of the heave in the aluminum cell [8].

Table II. MHD parameters in the metal pad

Parameters	Case 1	Case 2	Case 3
Average velocity (cm•s^{-1})	3.4	2.1	1.7
Maximum velocity (cm•s^{-1})	14.2	12.6	9.0
Percentage above 8 cm•s^{-1}	13.5	2.14	1.13
Percentage below 3 cm•s^{-1}	33.8	65	69.8
Metal heave (cm)	2.72	1.45	1.26

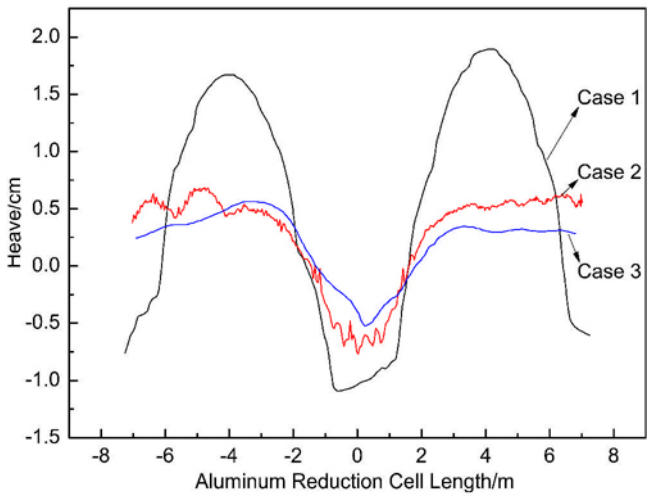

Figure 7. Wave curve of metal-bath interface at 1/2 width, x-axis

Figure 7 shows wave curve of metal-bath interface at 1/2 width, x-axis. The heaves of three cases are 2.72 cm, 1.45 cm, 1.26 cm respectively. Metal heave is reduced by 1.36 cm due to inclination and protrusions.

Conclusion

A three-dimensional (3-D) model was developed to study the influence of cathode shape on current density, electromagnetic force and metal heave in 300 kA aluminum reduction cell. Electromagnetic field and flow field were calculated in ANSYS and CFX. Results show that compared to plane cathode, cathode with 4.5° inclination can decrease 44.7 pct of horizontal current density. Cathode with 4.5° inclination and cylindrical protrusions can decrease 32.5 pct of horizontal electromagnetic force and 1.36 cm of metal heave in the metal pad.

Acknowledgements

The authors are grateful for the financial support by the National Nature Science Foundation of China (Grant No.50934005, No. 51204044 and No. 51434005).

References

1. N. Kandev, H. Fortin, "Electrical Losses in the Stub-anode Connection: Computer Modeling and Laboratory Characterization, " *TMS Light Metals*, (2009), 1061-1066.
2. T. Sele, "Instabilities of the metal surface in electrolytic alumina reduction cells," *Metallurgical Transactions B*, 8(4) (1977), 613-618.
3. X. Liang, "Busbar design of modern large aluminum reduction cell." *Light Metals*(in Chinese), (1990),20-26.
4. M. Li, "Research on the Numerical Simulation and Optimization of Magnetohydrodynamic Stability and Busbar Configuration in Aluminum Electrolysis Cell." (Ph.D. thesis, Central South University in China, 2007), 5-6.
5. Amit Gupta et al., "Electromagnetic and MHD study to improve cell performance of and end-to-end 86 kA potline." *TMS Light Metals*, (2012), 853-858.
6. W. Tao et al., "Numerical Simulation Electric Distribution In Aluminum Reduction Cell with Vertical Collector Bars," *METALURGIJA*, 53(1) (2014), 17-20.
7. Y. Liu et al., "Simulation and optimization of bus structure and electro-magneto-flow field of aluminum reduction cells with vertical bottom bars," *The Chinese Journal of Nonferrous Metal*, (2011), 1688-1695.
8. Subrat Das, Geoffrey Brooks and Yos Morsi, "Theoretical Investigation of the Inclined Sidewall Design on Magnetohydrodynamic (MHD) Forces in an Aluminum Electrolytic Cell," *Metallurgical and Materials Transactions B*, 42B (2011), 243-253.
9. B. Li et al., "Study of Electromagnetic Field in 300 kA Aluminum Reduction Cell with Innovation Cathode Structure," *TMS Light Metals*, (2011),1029-1033.
10. S. Das, G Littlefair, "Current Distribution and Lorentz Field Modeling Using Cathode Design: a Parametric Approach," *TMS Light Metals*, (2011), 847-851.
11. B. Li et al., "Modeling of Interface of Electrolyte/aluminum Melt in Aluminum Reduction Cell with Novel Cathode Structure," *TMS Light Metals*, (2012), 865-868.
12. R. Von Kaenel, J. Antille, "Modeling of Energy Saving by Using Cathode Design and Inserts," *TMS Light Metals*, (2011),569-574.
13. M. Dupuis, "Development of a 3D Transient Thermal-electric Cathode Panel Erosion Model of an Aluminum Reduction Cell," *TMS Light Metals*, (2000), 169-178.
14. J. Dreyfus, L Rivoaland and S. Lacroix, "Variable Resistivity Cathode against Graphite Erosion," *TMS Light Metals*, (2004), 603-608.
15. Mathieu Blais, Martin Désilets and Marcel Lacroix, "Optimization of the cathode block shape of an aluminum electrolysis cell," *Applied Thermal Engineering*, (2013), 439-446.
16. J. Li, C. Yin and H. Zhang, "Comparison of Some Different Cathode Collector Bars Through Numerical Simulation," *Light Metals*(in Chinese), (2013), 40-47.
17. Z. Ma, "Current Distribution at The Bottom of Aluminum Reduction Cell," *Light Metals*, (1986), 39-41.
18. Naixiang Feng. A cathode block structure that can reduce horizontal current in the metal of aluminum reduction cell: CN, 102400176A[P]. 2012-04-04.
19. Dagoberto S.Severo et al., "Modeling Magnetohydrodynamics of Aluminum Electrolysis Cells With Ansys and CFX, " *TMS Light Metals*, (2005), 475-480.